Research Article
Open Access

Analysis of Spatio-temporal environmental dynamics and vulnerability to land degradation in protected areas of Central India: insights from 1995 to 2025

Abstract

This study presents a multi-temporal, decadal assessment of land use land cover and environmental dynamics within four critical protected areas of Madhya Pradesh, India (*viz.* Bandhavgarh National Park (BNP), Kanha National Park (KNP), Satpura National Park (SNP), and Pench National Park (PNP). Utilizing a 30-year time series of Landsat satellite data (1995, 2005, 2015, and 2025), we evaluated the cascading impacts of land use/land cover (LULC) changes on Land Surface Temperature (LST), Normalized Difference Vegetation Index (NDVI), and subsequent land degradation vulnerability. The LULC analysis revealed an omnipresent trend of forest contraction and human footprint expansion across all four ecosystems. BNP experienced the sharpest net loss in forest/vegetation cover, decreasing by 37.0 km^2, while built-up areas expanded to account for 7.0% of the total landscape by 2025. KNP, SNP, and PNP exhibited similar trajectories, with forest areas shrinking by 20.1 km2, 26.56 km2, and 20.55 km2, respectively, heavily driven by encroaching agricultural activities and infrastructure development. Over the past 30 years, perennial surface water bodies have declined across all studied regions. Spatiotemporal regression analysis between NDVI and LST showed significant microclimatic shifts, with severely deforested areas exhibiting a strong inverse correlation between canopy density and land surface temperature, indicating pronounced localized warming. Predictive modeling using the Land Degradation Vulnerability Index (LDVI) further reveals that large portions of these habitats are under severe ecological stress. Even outside core protected zones, moderate-to-high degradation risks are widespread, driven by expanding agriculture and infrastructure, highlighting intensifying human pressure on forest ecosystems. Mirroring this trend, Kanha, Satpura, and Pench National Parks experienced forest contractions of 20.1 km², 26.56 km², and 20.55 km², respectively. These changes were primarily driven by agricultural expansion and infrastructure development. Furthermore, the multi-temporal assessment reveals a significant and simultaneous decline in perennial surface water bodies across all four conservation landscapes over the three-decade study period. These findings underscore the increasing anthropogenic pressure on these critical wildlife habitats and provide vital vulnerability metrics for future conservation and habitat management strategies.

Keywords: National parks, LST, LULC, NDVI, digital elevation model, remote sensing, GIS

Volume 9 Issue 1 - 2026

Tarun Kumar Thakur,[1] Digvesh Kumar Patel,[1] Jitendra Kumar,[1] Anita Thakur,[2] Priyanka Prakash[1]

[1]Department of Environmental Science, Indira Gandhi National Tribal University (IGNTU), India
[2]Krishi Vigyan Kendra, Indira Gandhi National Tribal University (IGNTU), India

Correspondence: Tarun Kumar Thakur, Department of Environmental Science, Indira Gandhi National Tribal University (IGNTU), Amarkantak (MP), India, 484887

Received: May 28, 2026 | **Published:** July 10, 2026

Abbreviations: LST, land surface temperature; LULC, land use and land cover; NDVI, normalized difference vegetation index

Introduction

Land degradation (LD) can be explored by evaluating various types of LULC, Soil health, plant diversity, Spectral vegetation indices using remote sensing and GIS techniques.[1] Expert judgment, techniques based on remote sensing, and analyses of changes in land cover are some of the assessment techniques used to evaluate land degradation. Since land degradation identification is by its very nature subjective and region-specific, remote sensing-based techniques are becoming the standard method for large-area investigations.[2] Continuous shifts in land use and land cover (LULC) have become a critical area of concern, primarily because of the ever-deepening relationship between human activities and ecological systems.[3] To address existing methodological inconsistencies in Land Use and Land Cover (LULC) research, this study implements an. LULC dynamics play a critical intensity analysis framework role in sustaining water resources, mitigating soil degradation, and regulating sediment transport in coastal systems.[4] Conversely, anthropogenic or natural shifts in these patterns trigger severe environmental repercussions, including global biodiversity decline, accelerated erosion, and hydrological cycle alterations. Furthermore, these structural transitions modify surface properties, ecosystem functions, and climatic patterns by disrupting the Earth's fundamental biogeochemical processes and energy balance.[5-7] Mitigating land degradation has become a top priority for scientists and policymakers because of its far-reaching consequences across environmental and socio-economic sectors. Consequently, reversing this decline is vital for realizing SDG 15.3, a target specifically dedicated to neutralizing desertification, restoring damaged terrains, and establishing sustainable land management practices.[8-10] Protected areas (PAs), including national parks, serve as critical focal points at the intersection of climate dynamics and sustainable development. These managed landscapes function as vital carbon reservoirs capable of sequestering substantial volumes of atmospheric carbon dioxide; however, they can conversely transition into carbon emitters if the organic carbon stored within vegetation and soil profiles is liberated back into the atmosphere.[11] By buffering ecosystems against intensive land-use modifications, national parks facilitate prolonged carbon sequestration within both biomass and soil layers over medium-to long-term horizons. Within these reserves, high floristic diversity maintains ecosystem productivity and enhances overall structural stability.[12] Protected areas are not entirely immune to human-

induced pressures and are increasingly vulnerable to shifting climatic regimes.[13-17] Consequences stemming from land use and land cover (LULC) dynamics present a significant challenge to the conservation efficacy and long-term viability of protected areas.[18] Concurrently, an extensive array of environmental and biophysical modeling frameworks depend heavily on high-precision, contemporary LULC datasets to facilitate robust resource allocation and strategic planning.[19-20] Systematic tracking of LULC transformations is therefore imperative for establishing sustainable landscapes and environmental stewardship. For instance, routine cartographic updates and multi-temporal remote sensing analyses can substantially enhance the monitoring of deforestation and land degradation rates in highly dynamic landscapes, such as those in West Africa, where rapid land cover transitions are common.[21,22] Global initiatives, including REDD+ (Reducing Emissions from Deforestation and Forest Degradation) and the UNCCD (United Nations Convention to Combat Desertification) "Zero Net Land Degradation" target, directly address these challenges. These frameworks promote targeted intervention strategies aimed at mitigating and reversing the widespread trends of desertification and forest loss.[23-25]

The magnitude and spatial distribution of Land Surface Temperature (LST) are governed by an interconnected suite of environmental variables, including land use/land cover (LULC) characteristics, topographic elevation, and the partitioning of thermodynamic fluxes into sensible and latent heat components.[26-28] To assess the vegetative drivers within this system, the Normalized Difference Vegetation Index (NDVI) has remained one of the most widely utilized remote sensing metrics since its inception in the 1970s. Driven by the expanding accessibility and enhanced resolution of satellite-derived Earth observation data, the scientific community routinely integrates NDVI into environmental modeling to quantify vegetation dynamics and subsequent thermal interactions.[29-30] In environmental assessment, integrating LST and NDVI metrics provides critical insights for mapping desertification pathways and formulating strategies for sustainable geo-environmental green growth, particularly in mitigating land degradation.

To implement this framework, a distinct thematic vector or raster layer was generated for each criterion using Geographic Information System (GIS) software. Within the spatial modeling environment, the attribution of layer weights varies by analytical context: under a natural vulnerability framework, all thematic criteria are allocated an identical, uniform weight. Conversely, when modeling environmental vulnerability, the assigned weights fluctuate dynamically to reflect the specific ecological sensitivity, operational significance, and localized utility of each theme layer within the study domain.[31] In contemporary environmental science, geospatial technologies have emerged as highly efficient and powerful instruments for tracking land-use dynamics, identifying species composition, and evaluating biological diversity within fragile tropical ecosystems.[1,32-34] These advanced geospatial frameworks provide reliable, objective, and empirical data essential for monitoring heterogeneous land-use systems, quantifying the spatial distribution of vegetation, and mapping rapid landscape modifications.[35-40]

Materials and methods

Study area

The selected national parks: Bandhavgarh National Park (1536.0 km²), Kanha National Park (940.0 km²), Satpura National Park (524.0 km²), and Pench National Park (257.03 km²) located in Madhya Pradesh and adjoining states, were chosen for this study. Multi-temporal satellite data for the years 1995, 2005, 2015, and 2025 were used to assess Land Use Land Cover (LULC), Normalized Difference Vegetation Index (NDVI), Land Surface Temperature (LST), and Land Degradation Vulnerability Index (LDVI) across four major LULC classes: water bodies, forest/vegetation, agricultural land, and built-up areas.

The geographical boundaries of the study sites are as follows:

Bandhavgarh National Park (BNP): 23°33'6.71"N to 23°43'2.78"N and 80°52'41.99"E to 81°04'47.59"E

Kanha National Park (KNP): 21°56'56.06"N to 22°22'11.70"N and 80°30'5.17"E to 81°01'31.34"E

Satpura National Park (SNP): 22°19'29.45"N to 22°35'41.92"N and 78°01'31.07"E to 78°22'31.50"E

Pench National Park (PNP): 21°32'57.46"N to 21°47'23.37"N and 79°10'49.93"E to 79°19'35.25"E

The mean elevation of the watersheds is 762 m (BNP), 864 m (KNP), 1325 m (SNP), and 681 m (PNP) above sea level. The geographic layout of the study domain and the locations of the selected national parks are illustrated through a Digital Elevation Model (DEM) in Figure 1. The region experiences a moderately humid tropical climate with distinct seasonal variations. A pronounced monsoon period brings heavy rainfall from July to September, followed by a pronounced dry season from April to June. A concise overview of the specific experimental protocols and technical workflows implemented to evaluate the diverse environmental parameters of this study is presented in the following subsections.

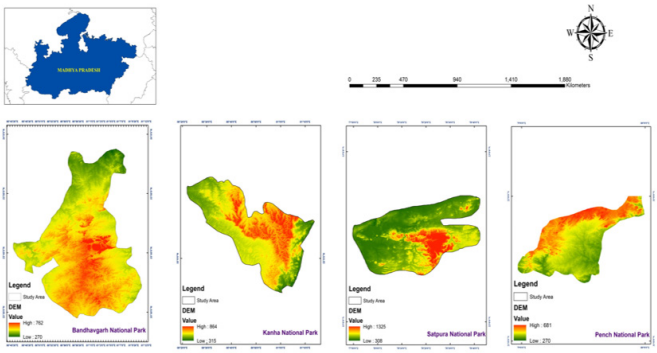

Figure 1 Layout map with digital elevation model of the study area.

Methodology

In the present study, Land Use/Land Cover (LULC) and land degradation dynamics were analyzed using integrated remote sensing and Geographic Information System (GIS) techniques. Satellite imagery was geometrically corrected and geo referenced using Survey of India (SOI) topographical maps at a scale of 1:50,000. The resulting maps were digitized, edited, and stored in ArcView GIS software. Drainage networks and stream ordering were automatically extracted using an ASTER Global Digital Elevation Model (DEM). The ASTER DEM datasets were downloaded from the USGS Earth Explorer portal and mosaicked to generate a seamless elevation surface covering the entire study area. The mosaicked DEM was subsequently processed in ArcGIS 10.3 using the Arc Data Management tools to delineate the study area boundary.

For Land Surface Temperature (LST) retrieval, thermal calibration constants and rescaling coefficients were obtained from the metadata files of each satellite scene. The overall methodological framework

of the study is illustrated in Figures 2-4. LST was derived using the SCP (Semi-Automatic Classification Plugin) in ArcGIS 10.3. Thermal Band 10 was used for LST estimation, while Bands 4 and 5 were employed to compute the Normalized Difference Vegetation Index (NDVI). Bands 2–7 were processed to generate the LULC raster layer, which was subsequently used to estimate surface emissivity values. Finally, linear regression models were developed to investigate the relationship between land cover characteristics and LST variations.

Selection of remote sensing data

For the present investigation, Landsat 3, 5, 7, and 8 satellite datasets corresponding to 1995, 2005, 2015, and 2025 were utilized (Table 1). The Landsat program, developed by the National Aeronautics and Space Administration (NASA), provides long-term Earth observation data for environmental and land resource studies. The satellite imagery used in this study was obtained from the USGS Earth Explorer platform managed by the United States Geological Survey (USGS). Digital image processing and analysis were carried out using ERDAS IMAGINE 2014 software on a personal computer, while secondary spatial datasets derived from Survey of India (SOI) topographical maps were processed and analyzed in ArcGIS. Elevation and contour information extracted from the SOI topo sheets were used to prepare various physiographic maps of the study area. Image enhancement techniques were applied to improve the visual quality of the satellite imagery and facilitate the identification of lineaments and other surface features. Initially, the geometrically corrected images were subjected to unsupervised classification using the classifier tool available in ERDAS IMAGINE 2014. Four preliminary spectral classes were generated in this stage. Subsequently, a supervised classification was performed to obtain more accurate land-use and land-cover categories. The classified signatures were refined and organized within the signature editor, and suitable color schemes were assigned to effectively represent different LULC classes.

Table 1 Characteristics of the selected Satellite data

Satellite	Sensor	Path/Row	Obtain date	Band used	Inclined angle	Swath width (Km)	Spatial resolution
Landsat 5	TM (Thematic Mapper)	143/044, 143/045, 145/044,	09/01/1995	Visible (B4, B5) NIR (B6 & B7)	99.1^0	185	80 m
Landsat 7	TM (Thematic Mapper)	143/044, 143/045, 145/044,	18/01/2005	Visible (B1, B2, B3,) NIR (B4) SWIR (B5), Thermal (B6)	98.2^0	185	30 m
Landsat 8	Enhanced Thematic Mapper Puls (ETM+)	143/044, 143/045, 145/044,	1/02/2015	Visible (B1, B2, B3,) NIR (B4) SWIR (B5), Thermal (B6)	98.2^0	185	30 m
Landsat 9	OLI-2/TIRS-2 (or OLI/TIRS)	143/044, 143/045, 145/044,	10/02/2025	Coastal aerosol(B1) Visible (B2, B3, B4) NIR (B5) SWIR- 1 (B6), SWIR -2 (B7)	98.2^0	185	15m

Preparation of land use land-cover classes

Land cover classification of the study area was performed using the Maximum Likelihood Algorithm (MLA) through a supervised classification approach. The resulting Land Use/Land Cover (LULC) maps are presented in Figure 2, which illustrates the decadal transformations observed in the study area over a forty-year period. The spatial and temporal variations among the different land-use categories are summarized in Table 2 and represented in Figure 3-5. In the supervised classification process, image pixels were assigned to specific land-use categories based on their spectral characteristics. The LULC pattern of the study area was broadly divided into four major classes: forest/vegetation, agricultural land, built-up areas, and water bodies.

Table 2 LULC changes in Various National Park

Bandhavgarh National Park									
		Area (%)							
Lulc Classes	**Area (K.m.^{2}) 1995**		**Area (K.m.^{2}) 2005**	**Area (%)**	**Area (K.m.^{2}) 2015**	**Area (%)**	**Area (K.m.^{2}) 2025**	**Area (%)**	**Difference 2025 Vs 1995 (km ^{2})**
Water Bodies	13.9	0.9	13.1	0.9	12.9	0.8	11.0	0.7	-2.9
Forest / Vegetation	1384.5	90.1	1379.0	89.8	1362.0	88.7	1347.5	87.7	-37.0
Agriculture	49.7	3.2	54.0	3.5	62.1	4.0	69.5	4.5	19.8
Built – up	87.9	5.7	89.9	5.8	99.0	6.4	108.0	7.0	20.1
Total	1536.0	100.0	1536.0	100.0	1536.0	100.0	1536.0	100.0	
Kanha National Park									

Lulc Classes	Area (K.m.²) 1995	Area (%)	Area (K.m.²) 2005	Area (%)	Area (K.m.²) 2015	Area (%)	Area (K.m.²) 2025	Area (%)	Difference 2025 Vs 1995 (km ²)
Water Bodies	7.1	0.8	6.3	0.7	5.6	0.6	4.2	0.4	-2.9
Forest / Vegetation	887.2	94.4	880.2	93.6	874.3	93.0	867.0	92.0	-20.1
Agriculture	6.9	0.7	9.8	1.0	11.1	1.2	14.3	1.5	7.4
Built – up	38.9	4.1	43.8	4.7	49.1	5.2	56.5	6.0	15.6
Total	940.0	100.0	940.0	100.0	940.0	100.0	942.0	100.0	

Satpura National Park

Lulc Classes	Area (K.m.²) 1995	Area (%)	Area (K.m.²) 2005	Area (%)	Area (K.m.²) 2015	Area (%)	Area (K.m.²) 2025	Area (%)	Difference 2025 Vs 1995 (km ²)
Water Bodies	4.12	0.79	3.60	0.69	2.93	0.56	2.18	0.42	-1.94
Forest / Vegetation	512.00	97.71	505.36	96.44	495.02	94.83	485.44	93.00	-26.56
Agriculture	2.62	0.50	4.02	0.77	8.01	1.53	13.25	2.54	10.63
Built – up	5.26	1.00	11.02	2.10	16.04	3.07	21.13	4.05	15.87
Total	524.00	100.00	524.00	100.00	522.00	100.00	522.00	100.00	

Pench National Park

Lulc Classes	Area (K.m.²) 1995	Area (%)	Area (K.m.²) 2005	Area (%)	Area (K.m.²) 2015	Area (%)	Area (K.m.²) 2025	Area (%)	Difference 2025 Vs 1995 (km ²)
Water Bodies	2.2	0.86	2.01	0.82	1.89	0.74	1.5	0.58	-0.7
Forest / Vegetation	249.9	97.23	243.65	94.79	236.58	92.04	229.35	89.23	-20.55
Agriculture	1.95	0.76	5.05	1.96	8.96	3.49	14.13	5.50	12.18
Built – up	2.98	1.16	6.32	2.46	9.6	3.73	12.05	4.69	9.07
Total	257.03	100.00	257.03	100.04	257.03	100.00	257.03	100	

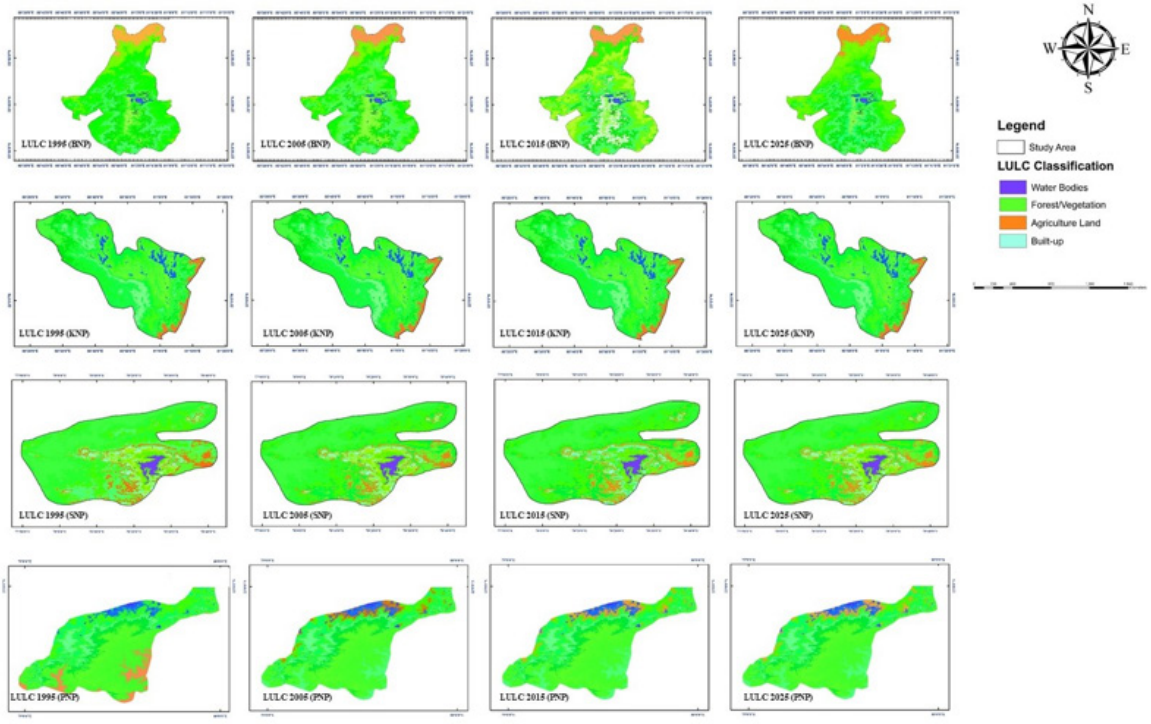

Figure 2 Comparative time-series maps displaying the classified habitat zones of Bandhavgarh, Kanha, Satpura, and Pench National Parks at 10-year intervals (1995, 2005, 2015, and 2025).

Citation: Thakur TK, Patel DK, Kumar J, et al. Analysis of Spatio-temporal environmental dynamics and vulnerability to land degradation in protected areas of Central India: insights from 1995 to 2025. *Biodiversity Int J.* 2026;9(1):28–38. DOI: 10.15406/bij.2026.09.00223

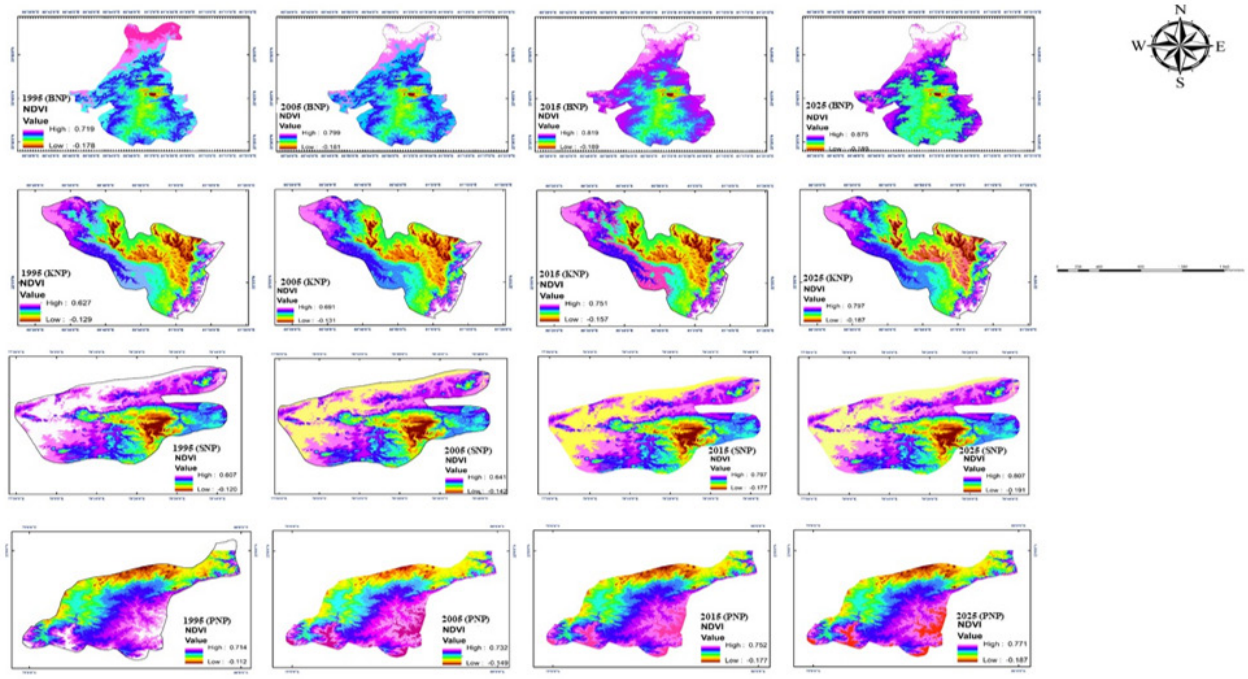

Figure 3 Normalized difference vegetation index (NDVI) maps illustrating changes across the study area from 1995 to 2025.

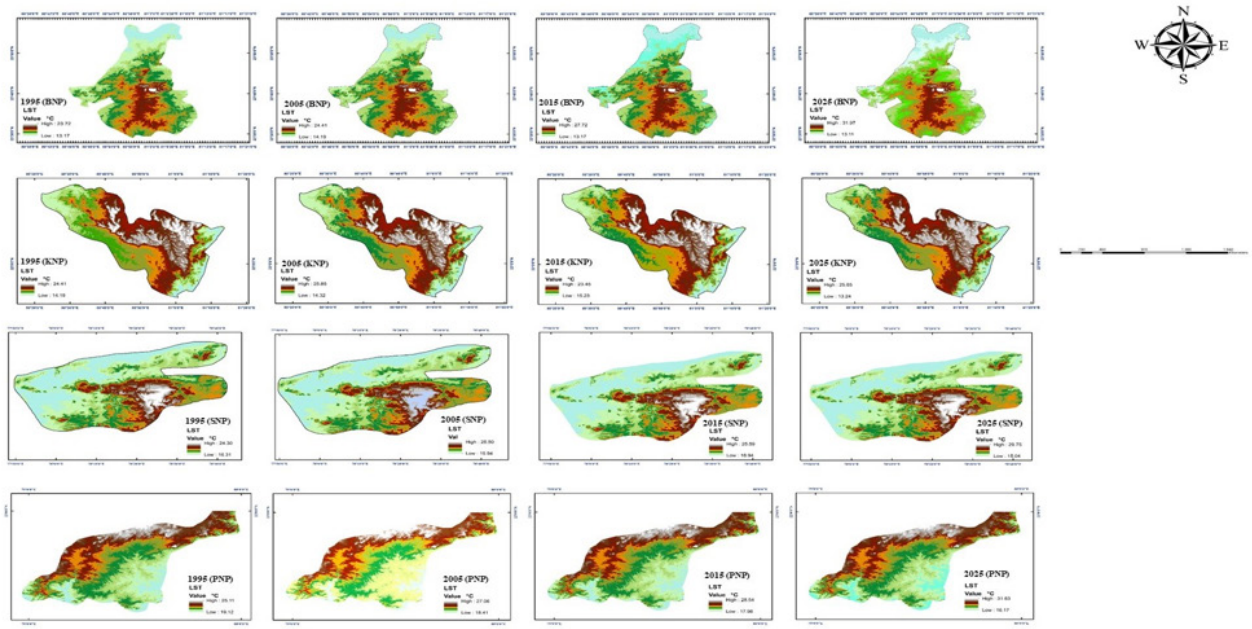

Figure 4 Spatiotemporal variations in land surface temperature (LST) within the study region across four selected years between 1995 and 2025.

Citation: Thakur TK, Patel DK, Kumar J, et al. Analysis of Spatio-temporal environmental dynamics and vulnerability to land degradation in protected areas of Central India: insights from 1995 to 2025. *Biodiversity Int J.* 2026;9(1):28–38. DOI: 10.15406/bij.2026.09.00223

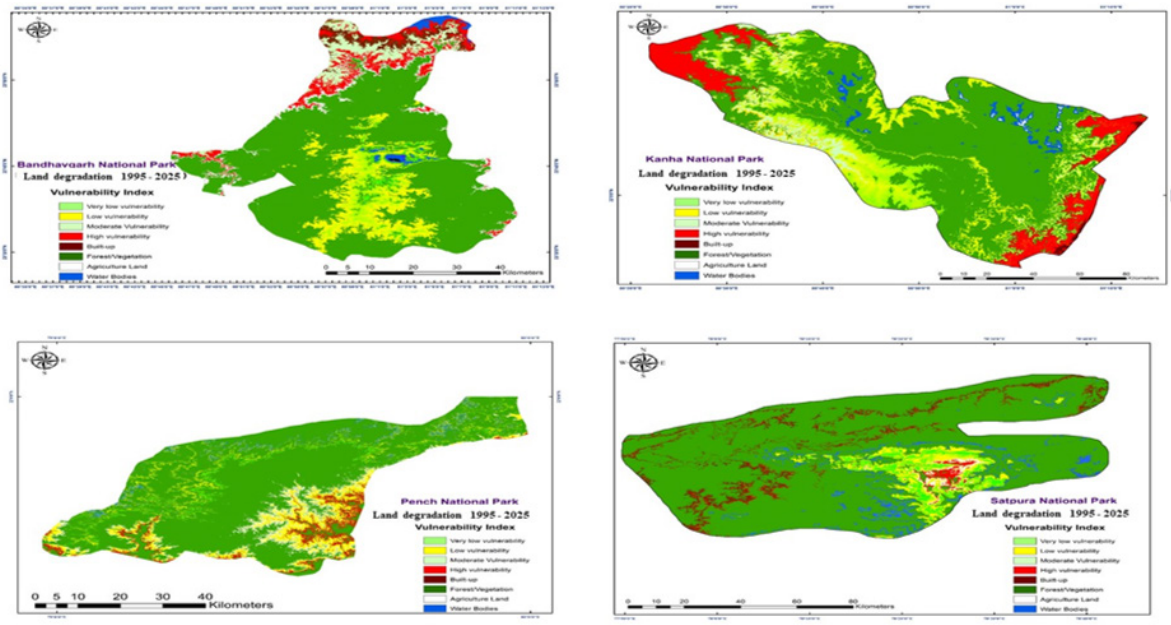

Figurer 5 Spatial distribution of the land degradation vulnerability index across the selected study region.

Vegetation mapping and calculation of spectral indices using NDVI

In the present study, vegetation mapping and forest health assessment for the period 1995–2025 were carried out using the Normalized Difference Vegetation Index (NDVI). This technique was applied to evaluate the temporal variations in vegetation density and overall forest conditions throughout the study period. The NDVI, derived from multispectral satellite imagery, is widely used to identify vegetation characteristics, analyze land use and land cover patterns, and detect environmental changes over time. The index also facilitated the discrimination of major surface features, such as forest and vegetation cover, agricultural land, water bodies, and built-up areas, using suitable spectral band combinations from satellite data. Earlier research has demonstrated that NDVI is an effective indicator for interpreting natural resources, particularly for monitoring vegetation conditions, assessing plant health, and examining LULC dynamics.[42] The Normalized Difference Vegetation Index (NDVI) is one of the most commonly used indicators for assessing vegetation conditions using remote sensing techniques. It is derived by combining the reflectance values of two spectral bands that are highly responsive to vegetation characteristics, namely the red (RED) and near-infrared (NIR) bands. The NDVI values generally range between −1 and +1, with higher positive values indicating dense and healthy vegetation cover. The NDVI can be calculated using the following equation[43-45] where: ρred and ρNir correspond to the reflectance of Red and near infrared bands of Landsat images, respectively.

Statistical analysis

In the present study, the correlation coefficient (R) was employed to evaluate the relationship between Land Surface Temperature (LST) and the Normalized Difference Vegetation Index (NDVI) for different study areas across each observation year, as illustrated in Figure 6. Two major indices, NDVI and LST, were analyzed to examine their spatial and temporal variations within the selected national parks. To establish measurable relationships between vegetation conditions and surface temperature, randomly selected independent pixels from the entire study area were used in the analysis.

Land Degradation Vulnerability Index (LDVI) model

To evaluate the cumulative impact of ground-level environmental stressors on landscape decline, the Land Degradation Vulnerability Index (LDVI) model was constructed by examining all permutations of the prioritized environmental classes. The distinct geospatial criteria variables governing land deterioration were integrated within a Geographic Information System (GIS) environment using the weighted overlay tool located under the ArcGIS Spatial Analyst toolbox, with their specific distribution.[38] A multi-criteria approach incorporating all combinations of the selected priority classes was adopted to develop the Land Degradation Vulnerability Index (LDVI) model. This model was designed to evaluate the combined influence of environmental and socioeconomic factors contributing to land degradation at the village level. Based on the LDVI assessment, the study area was categorized into different vulnerability zones, including very low, low, moderate, and high vulnerability. In addition, major land use and land cover categories, such as built-up areas, forests/vegetation, agricultural land, and water bodies, were identified and mapped within the analysis framework (Table 3 & Figure 5). Within the analysis framework, the study area was systematically classified into distinct vulnerability zones, ranging from very low to high. Furthermore, major land use/land cover (LULC) categories—specifically built-up areas, forest/vegetation, agricultural land, and surface water bodies—were identified and mapped to facilitate the assessment. As previously clarified, this spatial analysis is strictly limited to the four identified National Parks located within the state of Madhya Pradesh, India.

Table 3 Area under different categories of Land Degradation Vulnerability Index classes.

S.No.	Description	Bandhavghar National Parks (1995 - 2025)		Kanha National Parks (1995 - 2025)		Satpura National Park (1995 - 2025)		Pench National Park (1995 - 2025)	
		Area (Km^2)	Area (%age)	Area (Km^2)	Area (%age)	Area (Km^2)	Area (%age)	Area (Km^2)	Area (%age)
1	Very low vulnerability	6.6	8.2	1.85	4.0	2.35	4.27	1.4	3.2
2	low vulnerability	2.0	2.5	3.65	7.9	1.89	3.44	2.5	6.0
3	Moderate vulnerability	7.1	8.9	3.43	7.5	3.65	6.64	2.0	4.7
4	High vulnerability	1.6	2.1	0.4	0.9	0.65	1.18	0.7	1.7
5	Built – up	18.7	23.4	12.35	26.8	13.12	23.85	7.4	17.3
6	Forest /vegetation	24.4	30.5	17.54	38.1	25.2	45.82	18.4	43.2
7	Agriculture Land	17.5	21.9	5.36	11.7	7.21	13.11	9.7	22.8
8	Water Bodies	2.0	2.4	1.42	3.1	0.93	1.69	0.5	1.1
	Total	79.8	100	46	100	55	100	42.5	100

Result and discussion

Land use/land cover change from 1995 to 2025 (BNP)

Forest/vegetation, agricultural land, built-up areas, and water bodies were identified as the major LULC categories within Bandhavgarh National Park. The spatial and temporal distributions of these LULC classes for 1995, 2005, 2015, and 2025 are presented in Fig. 2, along with the statistical details of each category. In 1995, forest/vegetation represented the most dominant land cover class, occupying approximately 1384.5 km^2 (90.01%) of the total area, followed by agricultural land covering 49.7 km^2 (3.2%). Built-up land accounted for 87.9 km^2 (5.7%), and water bodies occupied 13.09 km^2 (0.9%) of the park area. In 2005, forest/vegetation continued to be the dominant category, although its area slightly declined to 1379 km^2 (89.9%) compared to 1995. In contrast, built-up land showed a marginal increase to 89.9 km^2 (5.8%). Agricultural land also expanded to 54 km^2 (3.5%), whereas water bodies slightly declined to 13.1 km^2 (0.9%), indicating conversion to other LULC categories. A similar trend was observed in 2015, when forest/vegetation still occupied the largest share of land, despite decreasing further to 1362 km^2 (88.7%). Built-up land increased to 99 km^2 (6.4%), and agricultural land expanded to 62.1 km^2 (4.0%). Water bodies declined slightly to 12.9 km^2 (0.8%), suggesting continued transformation into other land use categories. The same pattern persisted in 2025, with forest/vegetation remaining the dominant class but reducing to 1347.5 km^2 (87.7%). Built-up areas increased to 108 km^2 (7%), and agricultural land expanded to 69.5 km^2 (4.5%). Meanwhile, water bodies declined to 11 km^2 (0.7%) owing to conversion into other land use classes (Table 2). Overall, the study indicated that built-up land increased by approximately 20.1 km^2 between 1995 and 2025. Agricultural land also recorded an increase of approximately 19.8 km^2 during the same period. Conversely, forest/vegetation and water bodies decreased by nearly 37.0 km^2 and 2.9 km^2, respectively, reflecting their conversion into other LULC categories over time.

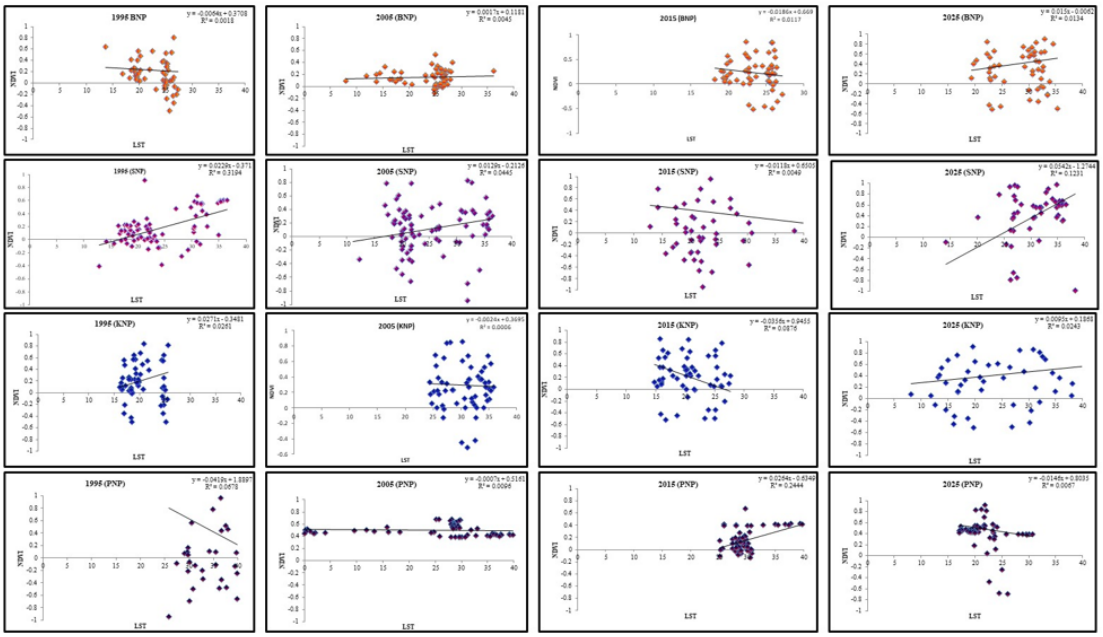

Figure 6 Spatiotemporal regression analysis of NDVI versus LST in various national parks (BNP, SNP, KNP, and PNP) from 1995 to 2025.

Land use/land cover change from 1995 to 2025 (KNP)

Forest/vegetation, agricultural land, built-up areas, and water bodies were identified as the principal LULC categories within Kanha National Park. The spatial and temporal distributions of these land use/land cover classes for 1995, 2005, 2015, and 2025 are presented in Figure 2, along with the statistical details of each category. In 1995, forest/vegetation was the dominant land cover class, occupying approximately 887.2 km² (94.4%) of the total area. Agricultural land covered approximately 38.9 km² (4.1%). The remaining portion of the park consisted of built-up land covering 38.9 km² (4.1%) and water bodies occupying 7.1 km² (0.8%) of the total area. In 2005, forest/vegetation continued to be the major LULC category, although its area slightly decreased to 880.2 km² (93.6%) compared to 1995. Conversely, built-up areas expanded marginally to 43.8 km² (4.7%). Agricultural land also increased, reaching 9.8 km² (1.0%), whereas water bodies declined to 6.3 km² (0.7%) due to conversion into other land use categories. A similar trend was observed in 2015, with forest/vegetation remaining the dominant class despite a further decline to 874.3 km² (93.0%). Built-up land increased to 49.1 km² (5.2%), and agricultural land expanded to 11.1 km² (1.2 km ²). Water bodies further reduced to 5.6 km² (0.6%), indicating continued transformation of land cover. The same pattern persisted in 2025, when forest/vegetation still represented the largest land cover class but declined to 864.0 km² (92.0%). Built-up areas increased to 56.5 km² (6.0%), and agricultural land expanded to 14.3 km² (1.5%). Water bodies decreased to 4.2 km² (0.4%) as parts of these areas were converted into other LULC categories (Table 2). Overall, the findings revealed a gradual increase in built-up land of approximately 15.6 km² between 1995 and 2025. Agricultural land also expanded by nearly 7.4 km² during the same period. In contrast, forest/vegetation and water bodies declined by approximately 20.1 km² and 2.9 km², respectively, reflecting their conversion into other land use and land cover classes over time.

Land use/land cover change from 1995 to 2025 (SNP)

Forest/vegetation, agricultural land, built-up areas, and water bodies were identified as the major LULC categories within Satpura National Park. The spatial and temporal distributions of these land use/land cover classes for 1995, 2005, 2015, and 2025 are presented in Figure 2, along with the statistical details of each category. In 1995, forest/vegetation was the dominant land cover type, occupying approximately 512.0 km² (97.71%) of the total area. Agricultural land covered approximately 2.26 km² (0.50%). The remaining portion of the park consisted of built-up land covering 5.26 km² (1.0%) and water bodies occupying 4.12 km² (0.79%) of the total area. In 2005, forest/vegetation continued to remain the major LULC class, although its extent slightly declined to 505.36 km² (96.44%) compared to 1995. In contrast, built-up land increased to 11.2 km² (2.10%). Agricultural land also expanded to 4.2 km² (0.77%), while water bodies decreased to 3.06 km² (0.69%) as portions of these areas were converted into other land use classes. A similar trend was observed in 2015, when forest/vegetation still represented the dominant category despite decreasing further to 495.02 km² (94.83%). Built-up areas increased to 16.04 km² (3.07%), and agricultural land expanded to 8.01 km² (1.53%). Water bodies declined slightly to 2.93 km² (0.56%), indicating continued land cover transformation within the park. The same pattern persisted in 2025, with forest/vegetation remaining the largest land cover class but declining to 485.44 km² (93.0%). Built-up land increased further to 21.13 km² (4.05%), and agricultural land expanded to 13.25 km² (2.54%). Water bodies decreased to 2.18 km² (0.42%) owing to conversion into other LULC categories (Table 2). Overall, the study revealed a gradual increase in built-up land of approximately 15.87 km² between 1995 and 2025. Agricultural land also increased by approximately 10.63 km² during the same period. In contrast, forest/vegetation and water bodies declined by nearly 26.56 km² and 1.94 km², respectively, reflecting their transformation into other land use and land cover classes.

Land-use/land-cover change from 1995 to 2025 (PNP)

Forest/vegetation, agricultural land, built-up areas, and water bodies were identified as the principal LULC categories within Pench National Park. The spatial and temporal distributions of these land use/land cover classes for 1995, 2005, 2015, and 2025 are presented in Figure 2, along with the statistical information for each category. In 1995, forest/vegetation was the dominant LULC class, covering approximately 249.9 km² (97.23%) of the total area. Agricultural land occupied approximately 1.95 km² (0.76%). The remaining area of the park consisted of built-up land covering 2.18 km² (1.16%) and water bodies occupying 2.2 km² (0.86%) of the total area. In 2005, forest/vegetation continued to be the major land cover category, although its extent declined slightly to 243.65 km² (94.79%) compared with 1995. Conversely, built-up areas increased to 6.32 km² (2.46%). Agricultural land also expanded to 5.05 km² (1.96%), whereas water bodies decreased to 2.01 km² (0.82%) owing to conversion into other land use categories. A similar trend was observed in 2015, when forest/vegetation remained the dominant class despite a further decrease to 236.58 km² (92.02%). Built-up land increased to 9.6 km² (3.73%), and agricultural land expanded to 8.96 km² (3.49%). Water bodies declined slightly to 1.89 km² (0.74%), indicating continued land cover transformation in the park area. The same pattern persisted in 2025, with forest/vegetation continuing as the largest LULC class but declining to 229.35 km² (89.23%). Built-up areas further increased to 12.09 km² (4.69%), and agricultural land expanded to 14.13 km² (5.50%). Water bodies declined to 1.5 km² (0.58%) as portions of these areas were converted into other LULC categories (Table 2). Overall, the study indicated that built-up land increased by approximately 9.07 km² between 1995 and 2025. Agricultural land also expanded by nearly 12.18 km² during the same period. In contrast, forest/vegetation and water bodies decreased by approximately 20.55 km² and 0.7 km², respectively, reflecting their conversion into other land use and land cover categories over time. The findings of the present study are consistent with observations reported in earlier research studies.[46-49]

Spatial-temporal patterns of canopy density

To evaluate the spatiotemporal changes in biomass vitality and greenness across the four studied protected areas—Bandhavgarh National Park (BNP), Kanha National Park (KNP), Satpura National Park (SNP), and Pench National Park (PNP)—a decadal Normalized Difference Vegetation Index (NDVI) analysis was conducted for the years 1995, 2005, 2015, and 2025 (Figure 3). The geographic distribution of NDVI values across a 30-year observation horizon highlights both natural phenological baselines and targeted areas of structural degradation. Analysis of the multi-temporal maps revealed that BNP's maximum NDVI values experienced a steady upward shift, climbing from 0.719 in 1995 to 0.799 in 2005, 0.819 in 2015, and reaching 0.875 by 2025. This incremental gain indicates the densification of the core forest canopies. However, the lowest spectrum of NDVI dipped from -0.178 (1995) to -0.245 (2025), indicating an increasing polarization of the landscape. This highlights that while core zones are consolidating, bare surfaces, built-up expansions, and degraded edges are becoming more starkly defined. The KNP demonstrated highly stable vegetative profiles. Its peak NDVI value moved progressively from 0.627 (1995) to 0.691 (2005), 0.751 (2015), and stabilized at 0.767 in 2025. Concurrently,

the lower boundary of the index dropped slightly from -0.129 to -0.187 over the three decades. The KNP demonstrated highly stable vegetative profiles. Its peak NDVI value moved progressively from 0.627 (1995) to 0.691 (2005), 0.751 (2015), and stabilized at 0.767 in 2025. Concurrently, the lower boundary of the index dropped slightly from -0.129 to -0.187 over the three decades. The spatial distribution indicates a highly contiguous, high-density vegetative block in the central and northern interiors, which visually supports its low landscape vulnerability metrics. PNP features a robust, well-distributed canopy envelope that corroborates its position as a park with the highest percentage of forest cover (43.2%). The maximum NDVI values rose systematically from 0.714 in 1995 to 0.732 in 2005, 0.752 in 2015, and capped at 0.771 by 2025. The lower value bounds transitioned from -0.112 (1995) to -0.187 (2025), which were largely confined to localized peripheral pathways and seasonal water body boundaries.

Spatiotemporal distribution of LST and its variations with LULC types

The spatial distribution of Land Surface Temperature (LST) for the four study periods—1995, 2005, 2015, and 2025—is illustrated in Figure 4. The results indicated noticeable temporal variations in the LST across all the selected national parks.

In Bandhavgarh National Park, the maximum and minimum LST values recorded in 1995 were 23.72 °C and 13.17 °C, respectively. In 2005, the maximum temperature increased to 24.41 °C, whereas the minimum temperature reached 14.19 °C. In 2015, the maximum LST further increased to 27.72 °C, whereas the minimum value was 13.17 °C. By 2025, the highest and lowest LST values were 37.97 °C and 13.11 °C, respectively. Similarly, in Satpura National Park, the maximum and minimum LST values in 1995 were 24.30 °C and 16.31 °C, respectively. In 2005, these values changed to 25.50 °C and 15.94 °C, respectively. In 2015, the maximum LST was 25.59 °C, whereas the minimum temperature was 18.94 °C. In 2025, the maximum and minimum LST values were 29.75 °C and 15.04 °C, respectively. In KNP, the maximum and minimum LST values during 1995 were 24.41 °C and 14.19 °C, respectively. In 2005, the maximum LST increased to 25.85 °C, whereas the minimum value was 14.32 °C. In 2015, the maximum and minimum LST values were 23.45 °C and 15.23 °C, respectively. By 2025, the maximum LST remained at 25.85 °C, whereas the minimum temperature declined slightly to 13.24 °C. In Pench National Park, the maximum and minimum LST values in 1995 were 25.11 °C and 19.12 °C, respectively. In 2005, the values increased to 27.06 °C and 18.41 °C, respectively. In 2015, the maximum LST was 28.54 °C, whereas the minimum value was 17.96 °C. In 2025, the highest and lowest LST values were 31.63 °C and 16.17 °C, respectively. The findings revealed that the central portions of all study areas experienced relatively higher LST values, whereas temperatures gradually decreased toward the peripheral regions. This spatial variation is mainly associated with the expansion of built-up areas and other impervious surfaces, which contribute significantly to the increase in surface temperature.[50-51]

Assessment of land degradation vulnerability index (LDVI) across protected areas

The quantitative distribution of the Land Degradation Vulnerability Index (LDVI) classes alongside major Land Use/Land Cover (LULC) features is structured to isolate zones under immediate ecological threat (Table 3 & Figure 5). The empirical assessment of the Land Degradation Vulnerability Index (LDVI) across the four protected areas from 1995 to 2025 reveals distinct environmental vulnerability patterns across the region. The spatial extent of degradation risk varies noticeably among the evaluated landscapes. Among the evaluated conservation systems, Bandhavghar National Park exhibits the highest relative vulnerability footprint, with 1.6 km^2 accounting for 2.1% of its total geographic extent categorized under severe degradation risk. This is followed by Pench National Park, which registers 0.7 km^2 (1.7%) within the high vulnerability zone. Conversely, KNP demonstrates the lowest severe risk exposure, restricting high vulnerability to a minor 0.4 km^2 (0.9%) footprint. For SNP, the high vulnerability class encompasses 0.9 km^2, representing a proportionate share of 0.65% of its landscape matrix. Moderate land degradation risk is widespread across all four parks, indicating ecosystems under transitional stress. Bandhavgarh National Park (BNP) records the largest area in this category (7.1 km² or 8.9%), followed by Satpura National Park (SNP) at 7.5 km² (3.65%), Kanha National Park (KNP) at 3.43 km² (7.5%), and Pench National Park (PNP) at 2.0 km² (4.7%). Areas with strong ecological resistance (very low and low vulnerability) are critical for core habitat protection. BNP supports the largest stable zone at 8.6 km² (10.7%). KNP has 5.5 km² of stable areas (very low: 1.85 km² / 4.0%; low: 3.65 km² / 7.9%), while PNP has 3.9 km² (very low: 1.4 km² / 3.2%; low: 2.5 km² / 6.0%). SNP shows 4.0 km² (2.35%) under very low vulnerability and 7.9 km² under low vulnerability. Dense forest and vegetative cover serve as the primary defense against soil erosion and runoff. PNP exhibits the highest proportion at 43.2% (18.4 km²), followed closely by KNP at 38.1% (17.54 km²). In comparison, Bandhavgarh National Park (BNP) has the lowest relative forest canopy cover at 30.5%, despite supporting the largest absolute forest area (24.4 km²). Satpura National Park (SNP) follows with 38.1 km² of forest and vegetative cover, representing 25.2% of its total area. Surface water bodies remain a limited but ecologically vital resource across these landscapes. Kanha National Park (KNP) records the highest proportion of open water at 1.42 km² (3.1%), followed by BNP at 2.0 km² (2.4%), Pench National Park (PNP) at 0.5 km² (1.1%), and SNP at 3.1 km² (0.93%). Among the four parks, BNP is the largest (79.8 km²), followed by SNP (55 km²), KNP (46 km²), and PNP (42.5 km²). Importantly, the summation of all LULC classes and vulnerability layers across the parks consistently totals 100%, confirming the statistical integrity and consistency of the multi-temporal satellite datasets used for assessing long-term land degradation trajectories in Central India.

Correlation of LST with NDVI data

The study indicated that most areas within the national parks showed lower NDVI values, whereas regions covered by dense vegetation recorded comparatively higher NDVI values. This pattern suggests an inverse relationship between NDVI and Land Surface Temperature (LST), as the central and more developed areas exhibited relatively higher LST values. Hence, NDVI was found to be negatively correlated with LST, implying that increasing urbanization significantly influences the surface thermal environment. The analysis further demonstrated a notable correlation between NDVI and LST with correlation coefficients of ($r = 0.0018$, 0.0045, 0.0117, and 0.0134 for BNP during 1995, 2005, 2015, and 2025, respectively), ($r = 0.03194$, 0.0445, 0.0049, and 0.1231 for SNP), ($r = 0.0261$, 0.0006, 0.0876, and 0.0243 for KNP), and ($r = 0.0678$, 0.0096, 0.2444, and 0.0067 for PNP), as presented in Fig. 6. The findings obtained in the present investigation are therefore consistent with the outcomes reported in earlier studies.[54-58]

Conclusion

This investigation assesses landscape changes, microclimatic variations, and eco-environmental vulnerabilities over three decades (1995-2025) in four protected areas of Madhya Pradesh, India:

Bandhavgarh National Park, Kanha National Park, Satpura National Park, and Pench National Parks. Combining multi-spectral Landsat data with geospatial indices, it reveals significant anthropogenic impacts, including a consistent decrease in forest canopy and an increase in human activity. BNP faced the most severe degradation, losing 37.0 km² of forest, while built-up areas expanded to 7.0% by 2025. Similar losses were noted in the other parks, driven by agriculture and ecotourism. Diminishing water bodies and altered Land Surface Temperatures indicate destabilized microclimates, with a strong inverse relationship between vegetation density and thermal emissions. Predictive modeling highlights widespread ecological stress across these regions, with agriculture and infrastructure developments threatening corridors and biodiversity, despite varying resilience levels among the parks.

Acknowledgements

None

Conflicts of interest

All authors declared that there is no conflicts of interest.

References

1. Duan X, Chen Y, Wang L, et al. The impact of land use and land cover changes on the landscape pattern and ecosystem service value in Sanjiangyuan region of the Qinghai–Tibet Plateau. *J Environ Manage.* 2023;325:116539.
2. Thakur TK, Padwar GK, Patel DK, et al. Monitoring land use, species composition and diversity of moist tropical environ in Achanakmaar Amarkantak Biosphere Reserve, India using satellite data. *Biodiversity Int J.* 2019;3(4):162–172.
3. Thakur T, Swamy SL, Thakur A, et al. Land cover changes and carbon dynamics in central India's dry tropical forests: A 25–year assessment and nature–based eco–restoration approaches. *J Environ Manage.* 2024;351:119809.
4. Aldwaik SZ, Pontius RG. Intensity analysis to unify measurements of size and stationarity of land changes by interval, category, and transition. *Landscape Urban Plan.* 2012;106(1):103–114.
5. Thakur TK, Dutta J, Bijalwan A, et al. Evaluation of decadal land degradation dynamics in old coal–mines of central India. *Land Degrad Dev.* 2022;33(16):3209–3230.
6. Ridding LE, Watson SC, Newton AC, et al. Ongoing, but slowing, habitat loss in a rural landscape over 85 years. *Landscape Ecol.* 2020;35:257–273.
7. Dimobe K, Goetze D, Ouedraogo A, et al. Spatio–temporal dynamics in land use and habitat fragmentation within a protected area dedicated to tourism in a Sudanian Savanna of West Africa. *J Landscape Ecol.* 2017;10.
8. Thakur TK, Patel DK, Thakur A, et al. Evaluation of land degradation vulnerability in coal mined areas of Madhya Pradesh, India using geospatial and AHP modeling: A 40–year assessment and eco–restoration of degraded landscape. *Environ Sustain.* 2025.
9. Thakur TK, Swamy SL, Bijalwan A. Assessment of biomass and net primary productivity of a dry tropical forest using geospatial technology. *J For Res.* 2019;30(1):157–170.
10. Herold M, Román–Cuesta RM, Mollicone D, et al. Options for monitoring and estimating historical carbon emissions from forest degradation in the context of REDD+. *Carbon Balance Manag.* 2011;6(1):13.
11. Dembele JB, Dimobe K, Konda B, et al. Modelling the current and future geographical distribution of *Combretum glutinosum* Perr. ex DC. under climate change in Burkina Faso: Future challenges and conservation opportunities. *J Nat Conserv.* 2025;86:126911.
12. Thakur TK, Patel DK, Thakur A, et al. Biomass production assessment in a protected area of dry tropical forest ecosystem of India: A field to satellite observation approach. *Front Environ Sci.* 2021;9:757976.
13. Knauer J, Zaehle S, Reichstein M, et al. The response of ecosystem water–use efficiency to rising atmospheric CO_2 concentrations: Sensitivity and large–scale biogeochemical implications. *New Phytol.* 2017;213(4):1654–1666.
14. Gonzalez P, Tucker CJ, Sy H. Tree density and species decline in the African Sahel attributable to climate. *J Arid Environ.* 2012;78:55–64.
15. Dimobe K, Ouedraogo A, Soma S, et al. Identification of driving factors of land degradation and deforestation in the Wildlife Reserve of Bontioli (Burkina Faso, West Africa). *Glob Ecol Conserv.* 2015;4:559–571.
16. Thakur TK, Patel DK, Thakur A, et al. Land degradation and ecological restoration in central India: A geospatial and machine learning analysis of coal mining impacts. *Trees For People.* 2025;21:100927.
17. Maynard DG, Paré D, Thiffault E, et al. How do natural disturbances and human activities affect soils and tree nutrition and growth in the Canadian boreal forest? *Environ Rev.* 2014;22(2):161–178.
18. Radeloff VC, Stewart SI, Hawbaker TJ, et al. Housing growth in and near United States protected areas limits their conservation value. *Proc Natl Acad Sci U S A.* 2010;107(2):940–945.
19. Forkuor G, Conrad C, Thiel M, et al. Integration of optical and synthetic aperture radar imagery for improving crop mapping in Northwestern Benin, West Africa. *Remote Sens.* 2014;6(7):6472–6499.
20. Patel DK, Thakur TK, Lal J. A spatio–temporal analysis of land use land cover changes of dry tropical forest ecosystem of Chhattisgarh, India. *Biodiversity Int J.* 2024;7(2):63–69.
21. Duadze SEK. *Land Use and Land Cover Study of the Savannah Ecosystem in the Upper West Region (Ghana) Using Remote Sensing.* Vol 16. Cuvillier Verlag; 2004.
22. Zoungrana BJ, Conrad C, Amekudzi LK, et al. Multi–temporal Landsat images and ancillary data for land use/cover change (LULCC) detection in the southwest of Burkina Faso, West Africa. *Remote Sens.* 2015;7(9):12076–12102.
23. Arora NK, Mishra I. Life on land: Progress, outcomes and future directions to achieve the targets of SDG 15. *Environ Sustain.* 2024;7(4):369–375.
24. Thakur TK, Dutta J, Upadhyay P, et al. Assessment of land degradation and restoration in coal mines of central India: A time series analysis. *Ecol Eng.* 2022;175:106493.
25. Wang J, Ai T, Wu H, et al. Graph–based spatial co–location pattern mining: Integrate geospatial analysis and logical reasoning. *Int J Digit Earth.* 2024;17(1):2390434.
26. Jamal S, Ahmad WS. Assessing land use land cover dynamics of wetland ecosystems using Landsat satellite data. *SN Appl Sci.* 2020;2:1891.
27. Barya MP, Kumar A, Singh B, et al. Utilization of constructed wetland for the removal of heavy metal through fly ash bricks manufactured using harvested plant biomass. *Ecohydrology.* 2022.
28. Kumar Y, Thakur TK, Thakur A. Socio–cultural paradigm of agroforestry in India. *Int J Curr Microbiol App Sci.* 2017;6(6):1371–1377.
29. Tariq A, Mushtaq A. Untreated wastewater reasons and causes: A review of most affected areas and cities. *Int J Chem Biochem Sci.* 2023;23:121–143.
30. Oke TR. The energetic basis of the urban heat island. *Q J R Meteorol Soc.* 1982;108:1–24.
31. Patel DK, Thakur TK, Thakur A, et al. Quantifying land degradation in upper catchment of Narmada River in central India: Evaluation study utilizing Landsat imagery. *Water.* 2024;16:2440.

32. Foody GM. Status of land cover classification accuracy assessment. *Remote Sens Environ.* 2002;80:185–201.

33. Venturini M, Franzetti B, Genovesi P, et al. Distribuzione e consistenza della popolazione di scoiattolo grigio *Sciurus carolinensis* Gmelin, 1788 nel levante genovese. *Hystrix.* 2005;16(1).

34. Mishra A, Swamy SL, Thakur TK, et al. Impact of coal mining on land use changes, deforestation, biomass and C losses in Central India: Implications for offsetting CO emissions. *Land Degrad Dev.* 2022.

35. Munsi M, Malaviya S, Oinam G, et al. A landscape approach for quantifying land–use and land–cover change (1976–2006) in middle Himalaya. *Reg Environ Change.* 2010;10:145–155.

36. Aksoy H, Kaptan S. Simulation of future forest and land use/cover changes (2019–2039) using the cellular automata–Markov model. *Geocarto Int.* 2022;37(4):1183–1202.

37. Patel DK, Thakur TK, Thakur A, et al. Groundwater potential zone mapping using AHP and geospatial techniques in the upper Narmada basin, central India. *Discov Sustain.* 2024;5:355.

38. Patel DK, Karuppannan S, Sao A, et al. Prioritization of sub–watersheds based on quantitative morphometric analysis of the Narmada River, India, using SRTM DEM and GIS techniques. *Biodiversity Int J.* 2024;7(1):22–33.

39. Thakur TK, Swamy SL, Dutta J, et al. Assessment of land use dynamics and vulnerability to land degradation in coal–mined landscapes of central India: Implications for ecorestoration strategies. *Front Environ Sci.* 2024;12:1419041.

40. Pandey M, Mishra A, Swamy SL, et al. Impact of coal mining on land use dynamics and soil quality: Assessment of land degradation vulnerability through conjunctive use of analytical hierarchy process and geospatial techniques. *Land Degrad Dev.* 2022;33:3310–3324.

41. Thakur TK. Diversity, composition and structure of understorey vegetation in the tropical forest of Achanakmaar Amarkantak Biosphere Reserve, India. *Environ Sustain.* 2018;1(2):279–293.

42. Bijalwan A, Verma P, Dobriyal MJR, et al. Trends and insight of agroforestry practices in Madhya Pradesh, India. *Curr Sci.* 2019;117(4):579–605.

43. Thakur U, Bisht NS, Kumar M, et al. Influence of altitude on diversity and distribution pattern of trees in Himalayan temperate forests of Churdhar Wildlife Sanctuary, India. *Water Air Soil Pollut.* 2021;232:205.

44. Ahmad A. Comparative analysis of supervised and unsupervised classification on multispectral data. *Appl Math Sci.* 2013.

45. Bhungeni O, Ramjatan A, Gebreslasie M. Evaluating machine–learning algorithms for mapping LULC of the uMngeni catchment area, KwaZulu–Natal. *Remote Sens.* 2024;16(12):2219.

46. Simwanda M, Ranagalage M, Estoque RC, et al. Spatial analysis of surface urban heat islands in four rapidly growing African cities. *Remote Sens.* 2019;11(14):1645.

47. Debele GB, Beketie KT. Monitoring the dynamics of land use and land cover, and their impact on seasonal land surface temperature in the Upper Awash Basin, Central Ethiopia. *Discov Appl Sci.* 2025;7(4):321.

48. Balew A, Korme T. Monitoring land surface temperature in Bahir Dar city and its surrounding using Landsat images. *Egypt J Remote Sens Space Sci.* 2020;23(3):371–386.

49. Arsiso BK, Tsidu GM, Stoffberg GH, et al. Influence of urbanization–driven land use/cover change on climate: The case of Addis Ababa, Ethiopia. *Phys Chem Earth.* 2018;105:212–223.

50. Thakur T, Thakur A. Litterfall patterns of a dry tropical forest ecosystem of Central India. *Eco Env Conserv.* 2014;20(3):1325–1328.

51. Liu P, Jia S, Han R, et al. RS and GIS supported urban LULC and UHI change simulation and assessment. *J Sens.* 2020;2020:5863164.

52. Simwanda M, Murayama Y, Phiri D, et al. Simulating scenarios of future intra–urban land–use expansion based on the neural network–Markov model: A case study of Lusaka, Zambia. *Remote Sens.* 2021;13(5):942.

53. Vani M, Prasad PRC. Assessment of spatio–temporal changes in land use and land cover, urban sprawl, and land surface temperature in and around Vijayawada city, India. *Environ Dev Sustain.* 2020;22(4):3079–3095.

54. Kumar Y, Thakur T. Agroforestry: Viable and futuristic option for food security and sustainability in India. *Int J Curr Microbiol App Sci.* 2017;6(7):210–222.

55. Dissanayake H, Vasilev VP, Khan S. Policies and strategies for a sustainable future. In: *Climate Neutrality Through Smart Eco–Innovation and Environmental Sustainability.* 2025:169.

56. Kumar Y, Thakur T, Sahu ML, et al. A multifunctional wonder tree: *Moringa oleifera* Lam. Open new dimensions in the field of agroforestry in India. *Int J Curr Microbiol App Sci.* 2017;6(8):229–235.

57. Dissanayake H, Vasilev VP, Khan S. A bibliometric analysis of alternative energy: Evaluating technologies, policies, and strategies for a sustainable future. In: *Climate Neutrality Through Smart Eco–Innovation and Environmental Sustainability.* Springer Nature Switzerland; 2025:169–191.

58. Mulualem GM, Liou YA. Application of artificial neural networks in forecasting a standardized precipitation evapotranspiration index for the Upper Blue Nile Basin. *Water.* 2020;12(3):643.